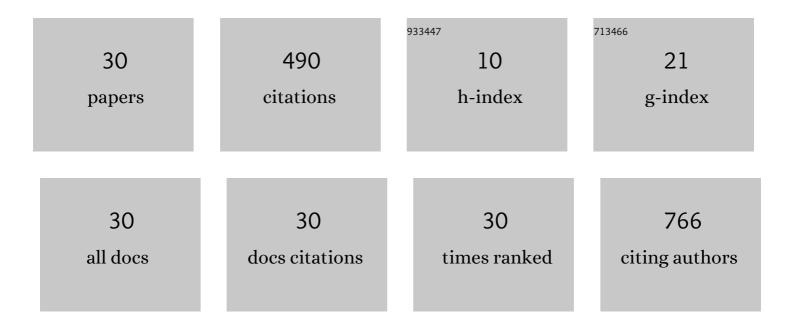
Sang Seo Park

List of Publications by Year in descending order

Source: https://exaly.com/author-pdf/11138475/publications.pdf Version: 2024-02-01



#	Article	IF	CITATIONS
1	Spatiotemporal inhomogeneity of total column NO ₂ in a polluted urban area inferred from TROPOMI and Pandora intercomparisons. GIScience and Remote Sensing, 2022, 59, 354-373.	5.9	4
2	Impacts of local versus long-range transported aerosols on PM10 concentrations in Seoul, Korea: An estimate based on 11-year PM10 and lidar observations. Science of the Total Environment, 2021, 750, 141739.	8.0	28
3	Investigation of the relationship between the fine mode fraction and Ãngström exponent: Cases in Korea. Atmospheric Research, 2021, 248, 105217.	4.1	4
4	A Possible Linkage between Dust Frequency and the Siberian High in March over Northeast Asia. Atmosphere, 2021, 12, 176.	2.3	8
5	Effect of solar zenith angle on satellite cloud retrievals based on O ₂ –O ₂ absorption band. International Journal of Remote Sensing, 2021, 42, 4224-4240.	2.9	3
6	Temperature Control of Spring CO2 Fluxes at a Coniferous Forest and a Peat Bog in Central Siberia. Atmosphere, 2021, 12, 984.	2.3	6
7	New Era of Air Quality Monitoring from Space: Geostationary Environment Monitoring Spectrometer (GEMS). Bulletin of the American Meteorological Society, 2020, 101, E1-E22.	3.3	165
8	Spatio-Temporal Variability of Aerosol Optical Depth, Total Ozone and NO2 Over East Asia: Strategy for the Validation to the GEMS Scientific Products. Remote Sensing, 2020, 12, 2256.	4.0	11
9	Synergistic Use of Hyperspectral UV-Visible OMI and Broadband Meteorological Imager MODIS Data for a Merged Aerosol Product. Remote Sensing, 2020, 12, 3987.	4.0	9
10	The implication of the air quality pattern in South Korea after the COVID-19 outbreak. Scientific Reports, 2020, 10, 22462.	3.3	43
11	Southern Hemisphere mid- and high-latitudinal AOD, CO, NO2, and HCHO: spatiotemporal patterns revealed by satellite observations. Progress in Earth and Planetary Science, 2019, 6, .	3.0	8
12	Effects of spatiotemporal O4 column densities and temperature-dependent O4 absorption cross-section on an aerosol effective height retrieval algorithm using the O4 air mass factor from the ozone monitoring instrument. Remote Sensing of Environment, 2019, 229, 223-233.	11.0	6
13	Simulation of Threshold UV Exposure Time for Vitamin D Synthesis in South Korea. Advances in Meteorology, 2019, 2019, 1-15.	1.6	3
14	Retrieval of NO2 Column Amounts from Ground-Based Hyperspectral Imaging Sensor Measurements. Remote Sensing, 2019, 11, 3005.	4.0	3
15	Changes in column aerosol optical depth and ground-level particulate matter concentration over East Asia. Air Quality, Atmosphere and Health, 2018, 11, 49-60.	3.3	25
16	Regional Characteristics of NO2 Column Densities from Pandora Observations during the MAPS-Seoul Campaign. Aerosol and Air Quality Research, 2018, 18, 2207-2219.	2.1	11
17	Characteristics of Classified Aerosol Types in South Korea during the MAPS-Seoul Campaign. Aerosol and Air Quality Research, 2018, 18, 2195-2206.	2.1	14
18	Effect of temperature-dependent cross sections on O4 slant column density estimation by a space-borne UV–visible hyperspectral sensor. Atmospheric Environment, 2017, 152, 98-110.	4.1	4

SANG SEO PARK

#	Article	IF	CITATIONS
19	Correlation analysis between regional carbon monoxide and black carbon from satellite measurements. Atmospheric Research, 2017, 196, 29-39.	4.1	7
20	Estimating Cloud and Aerosol UV Modification Factors Based on Spectral Measurement from the Brewer Spectrophotometer. Atmosphere, 2017, 8, 109.	2.3	6
21	Intercomparison of total column ozone data from the Pandora spectrophotometer with Dobson, Brewer, and OMI measurements over Seoul, Korea. Atmospheric Measurement Techniques, 2017, 10, 3661-3676.	3.1	10
22	Detection of Absorbing Aerosol Using Single Near-UV Radiance Measurements from a Cloud and Aerosol Imager. Remote Sensing, 2017, 9, 378.	4.0	3
23	Spectral dependence on the correction factor of erythemal UV for cloud, aerosol, total ozone, and surface properties: A modeling study. Advances in Atmospheric Sciences, 2016, 33, 865-874.	4.3	7
24	Utilization of O ₄ slant column density to derive aerosol layer height from a space-borne UV–visible hyperspectral sensor: sensitivity and case study. Atmospheric Chemistry and Physics, 2016, 16, 1987-2006.	4.9	20
25	Wavelength dependence of Ãngström exponent and single scattering albedo observed by skyradiometer in Seoul, Korea. Atmospheric Research, 2016, 181, 12-19.	4.1	13
26	Impact of UV-A radiation on erythemal UV and UV-index estimation over Korea. Advances in Atmospheric Sciences, 2015, 32, 1639-1646.	4.3	5
27	UV Sensitivity to Changes in Ozone, Aerosols, and Clouds in Seoul, South Korea. Journal of Applied Meteorology and Climatology, 2014, 53, 310-322.	1.5	8
28	Combined dust detection algorithm by using MODIS infrared channels over East Asia. Remote Sensing of Environment, 2014, 141, 24-39.	11.0	38
29	Inter-comparison of NO ₂ column densities measured by Pandora and OMI over Seoul, Korea. Korean Journal of Remote Sensing, 2013, 29, 663-670.	0.4	3
30	Sudden increase in the total ozone density due to secondary ozone peaks and its effect on total ozone trends over Korea. Atmospheric Environment, 2012, 47, 226-235.	4.1	15